Key Points:

- Anomalous responses of the ionospheric *F* layer over Brazil during a counter electrojet (CEJ) event
- Weakening and subsequent reversal of daytime equatorial electrojetss is noticed during a period of intense gravity wave (GW) activity
- The ionospheric F_2 layer stratification under a CEJ event probably due to the GW propagation

Correspondence to:

A. M. Santos,
angelamacsantos@gmail.com;
angelasantos_1@yahoo.com.br

Anomalous Responses of the F_2 Layer Over the Brazilian Equatorial Sector During a Counter Electrojet Event: A Case Study

A. M. Santos[1] , C. G. M. Brum[2], I. S. Batista[1], J. H. A. Sobral[1] , M. A. Abdu[1] , J. R. Souza[1] , S. S. Chen[1] , C. M. Denardini[1] , R. de Jesus[1] , K. Venkatesh[3], and P. A. B. Nogueira[4]

[1]National Institute for Space Research, São José dos Campos, Brazil, [2]Arecibo Observatory, University of Central Florida, Arecibo, Puerto Rico, [3]Physical Research Laboratory, Ahmedabad, India, [4]Federal Institute of Education, Science and Technology of São Paulo, Jacareí, Brazil

Abstract In this work, we report the ionospheric *F*-layer responses over the Brazilian equatorial sector to a counter electrojet event that occurred during the solar minimum period of June 2009. The data collected by the Digisonde over São Luis (2.33°S; 44°W; I: −4751°; Dip. Lat. 238°S) showed a strong modification in the ionospheric F_2 layer trace, which in this case appeared to be "broken in half." In this process, the first part of the F_2 layer (lower frequency) was thrown down whilst the upper part remained at higher altitudes. Such characteristics occurred simultaneously with an abrupt decrease in the strength of equatorial electrojet and with intensification in the auroral activity. The origin of this phenomenon seems to have a local nature and seems not to be connected to any magnetic disturbance since similar responses were not observed in other longitudinal and latitudinal sectors. Excluding this possibility, we assume that the strong changes observed in the *F* layer over São Luis had been caused probably by the gravity wave (GW) propagation, as seen in the downward phase propagation of the altitude contours with time over São Luis and Fortaleza and the remarkable signatures in ionograms over both regions, such as the forking traces that are typically caused by GWs.

1. Introduction

The day-to-day variability in the ionosphere is a phenomenon that is directly connected to the internal and external processes that modify the structure of the atmosphere-ionosphere-magnetosphere (AIM) system, such as internal atmospheric waves (gravity, planetary, tidal, and acoustic waves) that propagate to the ionosphere from the lower height regions (see e.g., Abdu, Batista, et al., 2006; Abdu, Ramkumar et al., 2006; Ghosh et al., 2019) and the magnetospheric solar and geomagnetic external forcing from above during the occurrence of disturbance space weather events (e.g., Abdu et al., 2003, 2009; Batista et al., 1991; Brum et al., 2021; Garzón et al., 2011; Kelley, 1989; Kelley et al., 2003; Kikuchi et al., 2008; Santos et al., 2012, 2016a, 2016b; Sastri et al., 1993; Sobral et al., 1997, 2001). Independently of the origin of the perturbations that arrive in the ionosphere, the variability occurring during the evening to post-sunset and night hours has gained special attention since the sunset electrodynamics processes play a fundamental role in the generation of important phenomena, such as the equatorial ionization anomaly and the plasma bubble irregularities (Abdu & Brum, 2009).

The vertically upwards propagating atmospheric waves have an important role in the coupling of the atmosphere-ionosphere system through wave saturation-dissipation processes since they carry energy and momentum, changing the background neutral wind and temperature (Vadas & Fritts, 2006; Yiğit & Medvedev, 2010) and consequently affecting the ionosphere (Vadas & Liu, 2009). As mentioned by Koucká Knížová et al. (2021), the ionospheric variability can be observed at a wide-scale temporal range that varies from minutes, or even shorter time scales, up to scales of the solar cycle and the secular variations of solar energy input. Although the general behavior of the ionosphere can be determined predominantly by the solar and geomagnetic forcings, the propagation of the lower atmospheric waves up to the ionosphere can contribute significantly to this variability.

Using different instruments, Ghosh et al. (2019) observed a long-period oscillation in the ionospheric parameters over Gadanki (13.5°N, 79.2°E, 6.5°N mag. lat.), a low latitude station in India during the solar minimum of 2009. They noted that waves ascending from the troposphere might have been the cause of the ionospheric variability over this region and that the *E* layer peak plasma frequency was directly connected to the equatorial electrojet (EEJ) strength. The gravity waves (GWs) influence in the equatorial spread *F* irregularity development

during post sunset hours was investigated by Abdu (2012), showing evidence that the tropospheric GWs can be an important cause of the spread *F* day-to-day variability. The author mentioned that the GWs wind perturbations could contribute to the instability growth both through the density modulation (possibly from the meridional wind component) as well as due to the generation of polarization electric field (from the zonal and vertical wind components). Fritts et al. (2008) reported the impacts of GWs and tidal perturbations on the bottom side *F* layer. They observed that such perturbations appeared to have the potential to impact the plasma instability processes and the seeding of plasma bubbles.

Using data collected by the São Luís 30 MHz coherent scatter radar, Shume et al. (2014) studied the effect of the atmospheric waves at the *E* region heights over the Brazilian sector. They noticed an unusual quasiperiodic fluctuation in the intensity of the EEJ irregularities possibly caused by atmospheric waves. Based on GOES-8 satellite measurements, it was suggested that atmospheric gravity waves probably launched by the deep tropospheric convection activities were responsible for the decrease in the EEJ intensity over the equatorial region of São Luis. In agreement with the authors, GWs generated from these convection sources could have obliquely propagated to the *E* region and caused the horizontal magnetic field perturbations (a proxy for electrojet strength). As mentioned by Shume et al. (2014), gravity waves with a vertical wavelength of less than 50 km can interact with the background dynamo field in the electrojet and cause electric field variations with altitude.

Analyzing the dayglow photometer and magnetometer data over the equatorial Indian sector, Vineeth et al. (2012) showed the possible influence of the upward propagation of the gravity waves from mesosphere to lower thermosphere on the reversal of the vertical polarization electric field and hence in the counter electrojet (CEJ) events. A decrease in the wave activity in the mesopause temperature during and after CEJ occurrence time was noticed when a mesospheric zonal wind showed a reversal from west to east. This indicated strong vertical coupling between the mesopause and the dynamo region through the GW associated with vertical winds.

Different mechanisms have been proposed to explain the reversal of the EEJ current during morning and post-noon hours during quiet-time periods, such as the reversal of vertical polarization electric field caused by large vertical winds associated with gravity waves (Raghavarao & Anandarao, 1980); the formation of an additional current system by the interaction of altitude varying winds (Fambitakoye et al., 1976); and the reversal of zonal electric field by appropriate phase combination of global scale tidal wind modes (Gurubaran, 2002; Somayajulu et al., 1993). On the other hand, during disturbed periods, the formation of CEJ can be related to a combination of tidal variability, gravity waves, prompt penetration of electric fields of magnetospheric origin (Kikuchi et al., 2000), and also disturbance dynamo electric field (see Soares et al., 2018 and references therein).

The process associated with the reversal of the EEJ current can strongly impact the behavior of the equatorial ionosphere (see e.g., Abdu et al., 2017; Denardini et al., 2009; Kelley et al., 2009; Soares et al., 2018; Venkatesh et al., 2015). In this paper, we will investigate an interesting and anomalous response of the *F* region to a CEJ event registered over the Brazilian equatorial sector during the deep solar minimum of 2009, which although having occurred simultaneously with the beginning of a weak magnetic storm, seems not to be related to it. The possible influence of the GW as a precursor of such local variability over the equatorial ionosphere is discussed here.

2. Results

Observational data collected by the Digisondes operating at the Brazilian stations of São Luís (SL, 2.33°S, 44°W; I: −4.751°; Dip Lat. 2.38°S), Fortaleza (FZ, 3.73°S, 38.52°W; I: −13.443°; Dip Lat. 6.82°S) and Cachoeira Paulista (CP, 22.7°S, 45°W; I: −34.596°; Dip Lat. 19°S) are used to investigate the ionospheric conditions during the strong CEJ event that occurred on 28 June 2009. Panel a of Figure 1 shows the geophysical conditions as a function of universal time (UT) of the Sym-H index, the components *B*y and *B*z of the interplanetary magnetic field, the auroral electrojet activity index (AE), and a proxy for the strength of the EEJ based on the magnetometer observations over the Brazilian and Peruvian sectors. Panel b shows the observational locations used in this work and the location of the magnetic equator for the year 2009 (black line). The acronym CEJ and/or westward EEJ is used here to refer to the EEJ reversal from its normal eastward direction.

The diurnal variations of the EEJ over Brazil ($\Delta H_{SL} - \Delta H_{VS}$, red curve in the lower panel of Figure 1a) were calculated using the same methodology of Denardini et al. (2009), considering the difference between the *H* component
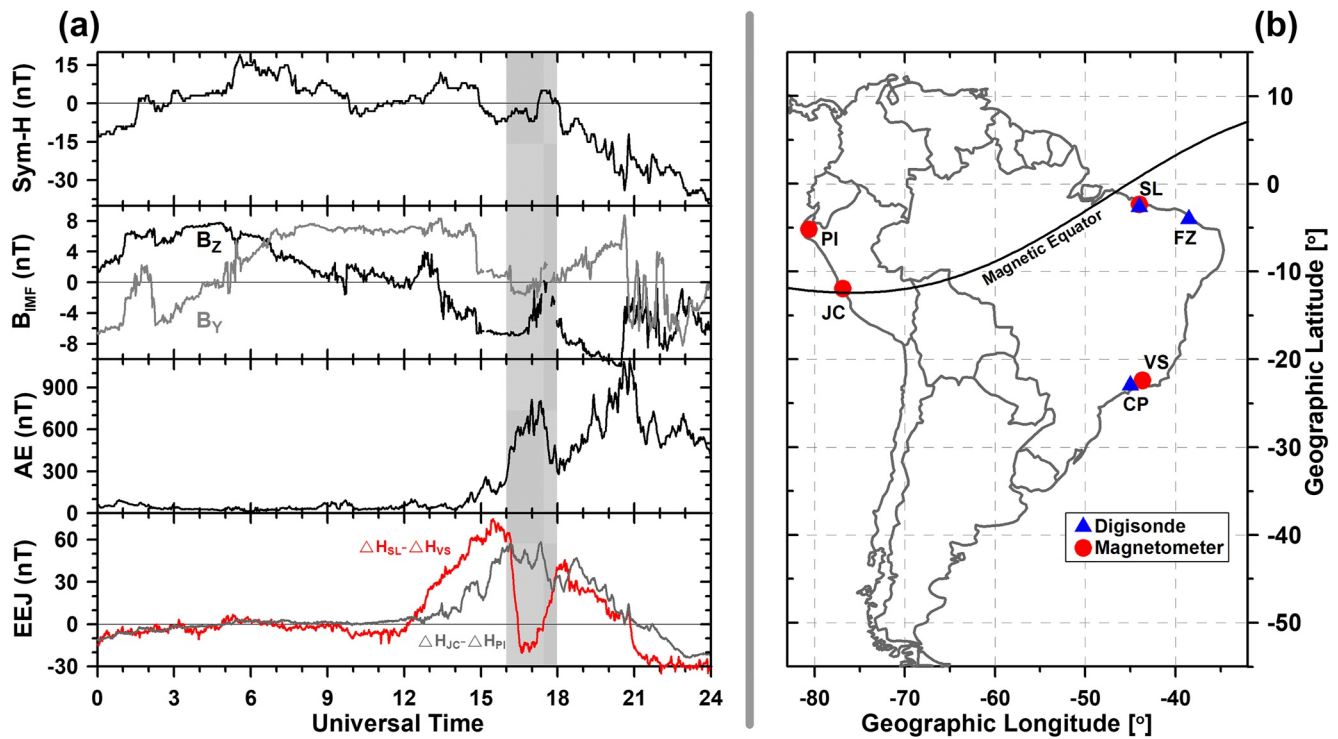
Figure 1. (a) From top to bottom panels. 1 minute values of Sym-H index; the interplanetary magnetic field components B_z and B_y (black and gray lines, respectively); the auroral activity index (AE), and the strength of equatorial electrojet (EEJ) over Brazil ($\Delta H_{SL}-\Delta H_{VS}$, red color) and over Peru ($\Delta H_{JC}-\Delta H_{PI}$, gray color) during 28 June 2009. (b) Map of South America showing the observational locations used in this study.

variations of the Earth' magnetic field over São Luís and Vassouras (VS, 22.40°S, 43.66°W; I: −35.387°; Dip Lat. 19.6°S). Over the Peruvian region ($\Delta H_{JC}-\Delta H_{PI}$, gray curve in the lower panel of Figure 1a) the calculation of EEJ was based on the data from Jicamarca (JC, 11.95°S, 76.87°W; I: 0.511; Dip Lat. 0.6°N) and Piura (PI, 5.17°S, 80.64°W; I: 12.964; Dip Lat. 6.57°N). The inclinations (I) and dip latitudes were calculated for SL, CP, FZ, VS, JC and PI (for the year 2010 at an altitude 300 km) using IGRF-13 (https://wdc.kugi.kyoto-u.ac.jp/igrf/point/index.html).The shaded area in Figure 1a indicates the period in which strong modifications were observed in the ionospheric equatorial region of São Luís (between 16:00 UT and 18:00 UT) as will be shown in the next figures. It can be observed that before this interval, the geomagnetic conditions were very quiet, as evidenced by the small variation in AE index and Bz northward or oscillating around zero (up to 13:30 UT). At 14:50 UT, a slight intensification can be seen in Bz, which is accompanied by a rapid decrease in By and a smoothed increase in AE index. Between 15:00 UT and 17:50 UT, Bz remained constant southward, and in the middle of this interval (~16:10 UT), the auroral activity presented an intensification, varying from 200 to 500 nT, which was simultaneous with an inversion of By to west. At the same time, the EEJ strength over Brazil presented a very strong decrease (~80 nT), and reverted to the west. No significant variation was observed over the Peruvian sector, which in this case presented only small fluctuations during the interval of interest, which makes us to believe that this CEJ event had a local origin.

Figure 2 shows the variations of the equatorial and low latitude ionospheric F-layer peak heights and critical frequency (panels b–d) over Brazil on 28 June 2009. The EEJ during this day (EEJ_{28June}) is again shown in the upper panel (panel a, red curve) together with the average quiet-time reference (EEJ_{ref}, blue curve) and the respective standard-deviations. Due to the absence of data for SL in June, we use only 27 June as representative of quiet-time day, whilst for the case of Vassouras, the average value of five quiet-days of June was used as reference to calculate the EEJ_{ref} as given by $EEJ_{ref} = \Delta H_{SL(27)} - \Delta H_{VS(av\ 5qds)}$. Comparing the curve of EEJ_{27June} (cyan dots), calculated as $EEJ_{27June} = \Delta H_{SL(27)} - \Delta H_{VS(27)}$, with the EEJ_{ref} (blue with error bars), it is possible to see only small differences, which indicates that the use of only 1 day over SL (day 27) was not a problem to define the quiet-time pattern. It is interesting to note that the EEJ on 28 June was lower than the reference curve
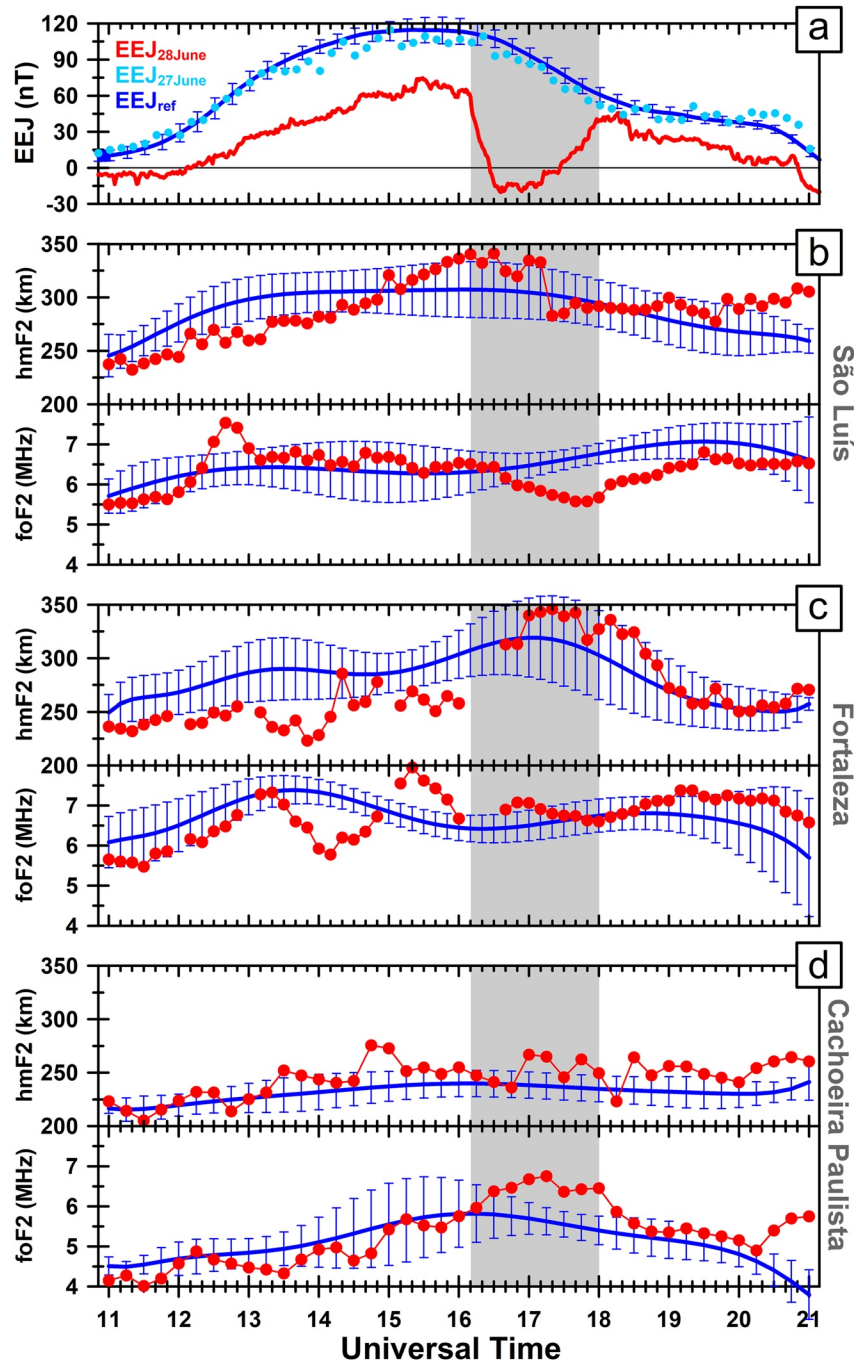
Figure 2. From top to bottom are shown: the equatorial electrojet (EEJ) strength over Brazil (panel a) during 27 (cyan dots) and 28 June 2009 (red curve) with the respective quiet-time reference (panel a, blue curve); F layer peak height–hmF_2 and the F_2 layer critical frequency–foF_2 (red dots) over SL (panel b), FZ (panel c) and CP (panel d). The average quiet days hmF_{2ref} and foF_{2ref} and their respective standard deviations are represented by the blue curves. The solid blue curves, indicated in panels b–d represent the smoothing made in average data, hmF_2 and foF_2 using polynomial interpolation. The plots are in function of universal time (UT = LT + 3 h).

during the entire period analyzed, mainly between 16:00 UT and 18:00 UT (shaded area) when the difference between the two curves was higher.

The variation of the F_2 layer peak height (hmF_2) and the critical frequency (foF_2) on 28 June (red dots) over SL, FZ, and CP and their respective quiet-time reference curve and standard deviations are shown in panels b–d of

Figure 2, respectively. The average curves for foF_2 and hmF_2 were calculated considering the same five quiet-days of June used in the definition of $\Delta H_{VS(av\ 5qds)}$, except for FZ, for which it was necessary to choose two different days due to the poor quality of data. In the case of quiet-time average values, we use a polynomial fitting for the smoothing process. It can be observed that hmF_2 over the regions near the equator (SL and FZ, panels b and c) presented a very atypical behavior on this day, being lower when compared to the average quiet days between ~11:00 UT and 15:00 UT in SL and ~11:00 UT and 16:00 UT in FZ. It can be noticed that this anomalous behavior of hmF_2 over SL and FZ is concurrent with the EEJ decrease during these hours, as can be seen by the red curve in panel a. It was noteworthy that near the CEJ occurrence time, an increase in hmF_2 was observed over SL (~15:00 UT). Over CP, the hmF_2 on 28 June was very similar to the reference curve, with only a few fluctuations.

Regarding the foF_2 parameter, Figure 2 shows an increase in SL near 12:20 UT and a decrease in the interval that followed the CEJ event and its recovery. An interesting modification in a wave-like pattern was observed in foF_2 over FZ between 13:00 UT and 16:00 UT. Finally, over CP, the most important variation in foF_2 was observed coinciding with the EEJ decrease at 16:10 UT. In this case, the foF_2 parameter on 28 June presented an increase when compared to its value on the quiet-days. Such increase was probably caused by the fountain effect, since there is an increase in hmF_2 over the equatorial region of SL (i.e., followed by a decrease in foF_2 over this same sector) ~1 h before the increase in foF_2 over the low latitude sector of CP.

Panel b of Figure 3 shows a set of eight selected ionograms to show the responses of the ionosphere over SL before, during, and after the CEJ event interval on 28 June along with the Brazilian EEJ strength over the same region as the reference (panel a). As can be seen, at 15:50 UT (20 minutes before the beginning of the decrease in EEJ), the Digisonde registered four different layers (ionogram 1), being two of them sporadic E (E_s) layers, located at about 100 (q or l-type) and 130 (c-type), the F_1 layer at ~200, and F_2 layer at ~430 km (note that all the heights mentioned here are the minimum virtual heights of each layer). Coinciding with the abatement of the EEJ the F_2 layer was strongly modified starting at 16:20 UT (ionogram 2) as shown by its trace which is spectacularly "broken in half," forming in this way two new layers. This discontinuity occurred simultaneously with an increase in the AE index and a reversal of B_y under continuous southward B_z (see Figure 1). From here on, we will refer to these two layers as F_2a and F_2b (bottom and upper layers, respectively).

It is interesting to observe in Figure 3b that at 15:50 UT, the F_1 layer minimum virtual height stays around 200 km, with group retardation/delay at foF_1, as indicated by the blue arrow in the curved trace of the ordinary wave (pink trace, ~4.3 MHz). The F_2 layer base height, $h'F_2$, at this same time is located at around 430 km. In ionogram 2 (16:20 UT), the structure of the upper layers was completely modified. Immediately after the CEJ occurrence, the F_1 layer that presented a critical frequency of ~4.3 MHz became a thick layer as indicated by the large group retardation at the beginning of the new F_2a layer (see the blue vertical rectangle in the frequency range of the ordinary trace between ~4.3 and 5 MHz e.g.,). This retardation occurs due to an increase in the group velocity (the velocity that transports wave energy) as the wave approaches the reflection height. In this case, the electromagnetic wave suffers a deceleration as it approaches the peak electron density. So, the larger the thickness of the lower layer, the higher will be the curvature in the trace of the upper layer at their lower frequency and, therefore, the higher will be the virtual height of this upper layer (for more details about radio-wave propagation see Ratcliffe, 1959 and Budden, 1985).

On the other hand, the F_2b layer at 16:20 UT appears to be a thin layer since there is no group retardation at its lower frequency (~5.3 MHz). At 16:30 UT, when the CEJ attained its minimum value of −20 nT (indicated by number 3), the top frequency of the F_2a increased to 5.7 MHz and the minimum virtual height of the F_2b increased (to 540 km) partly due to the blanketing caused by the F_2a (see ionogram 3). It was possible to follow this ascending movement of the F_2b layer until 17:10 UT (not shown here). After this, the F_2b layer is not seen in the ionogram, probably because it moved upward to beyond the Digisonde upper sounding limit, which was 800 km in the present case. As the CEJ intensified its recovery phase (numbers 5 and 6), the F_2a layer presented a stratification at the high frequency end (see the horizontal blue line in ordinary and extraordinary traces) that also moved further upward. After 18:10 UT, the ionosphere gradually returned to its normal behavior as can be seen in the ionograms numbered 7 and 8. During this period of intense changes in the F region over SL, it can be verified that the c-type Es layer mentioned previously (located at about 130 km in ionogram 1) merged with the lower Es layer (see ionogram sequences up to number 5). At 18:10 UT, a total blocking of these two layers was seen and a new configuration of Es layer was established.
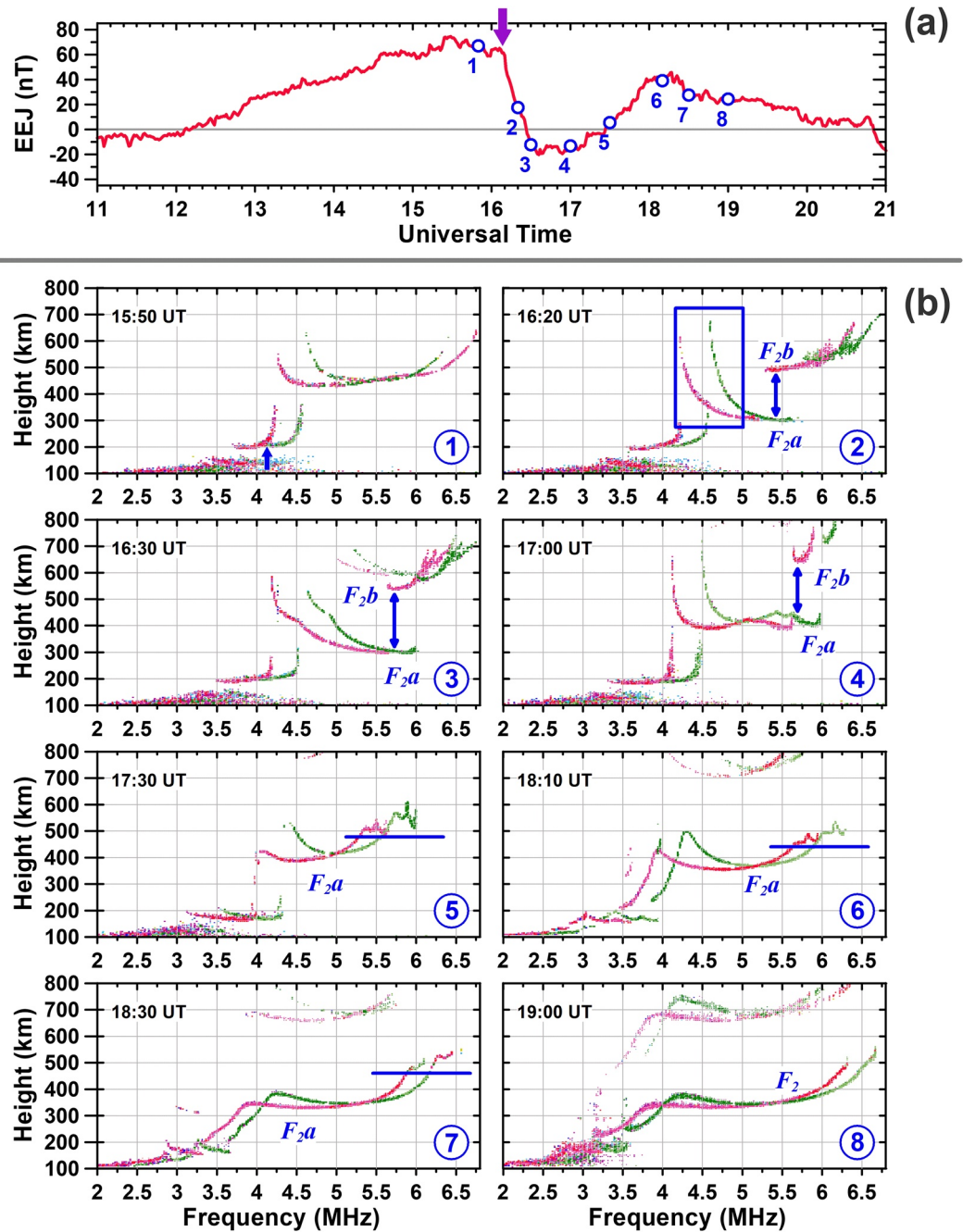
Figure 3. (a) The equatorial electrojet (EEJ) strength over Brazil. The numbers from 1 to 8 are used as a reference to indicate ionograms' changes over São Luís (for more details, see the text). (b) Ionograms over SL for some specific times of 28 June 2009.

3. Discussion

Based on the geomagnetic indices presented in Figure 1, it is improbable that this CEJ event could have been caused by disturbance electric fields of magnetospheric origin, mainly because of the following reasons: (a) at the beginning of the EEJ decrease, the AE index presented an increase, which would represent, at that local time, an eastward electric field under southward Bz condition. This electric field would cause an increase in EEJ (e.g., Venkatesh et al., 2017) and not the decrease as observed here; (b) an electric field of magnetospheric origin would have caused similar effects over the Peruvian sector, which is only 30° westward of the Brazilian sector, but the
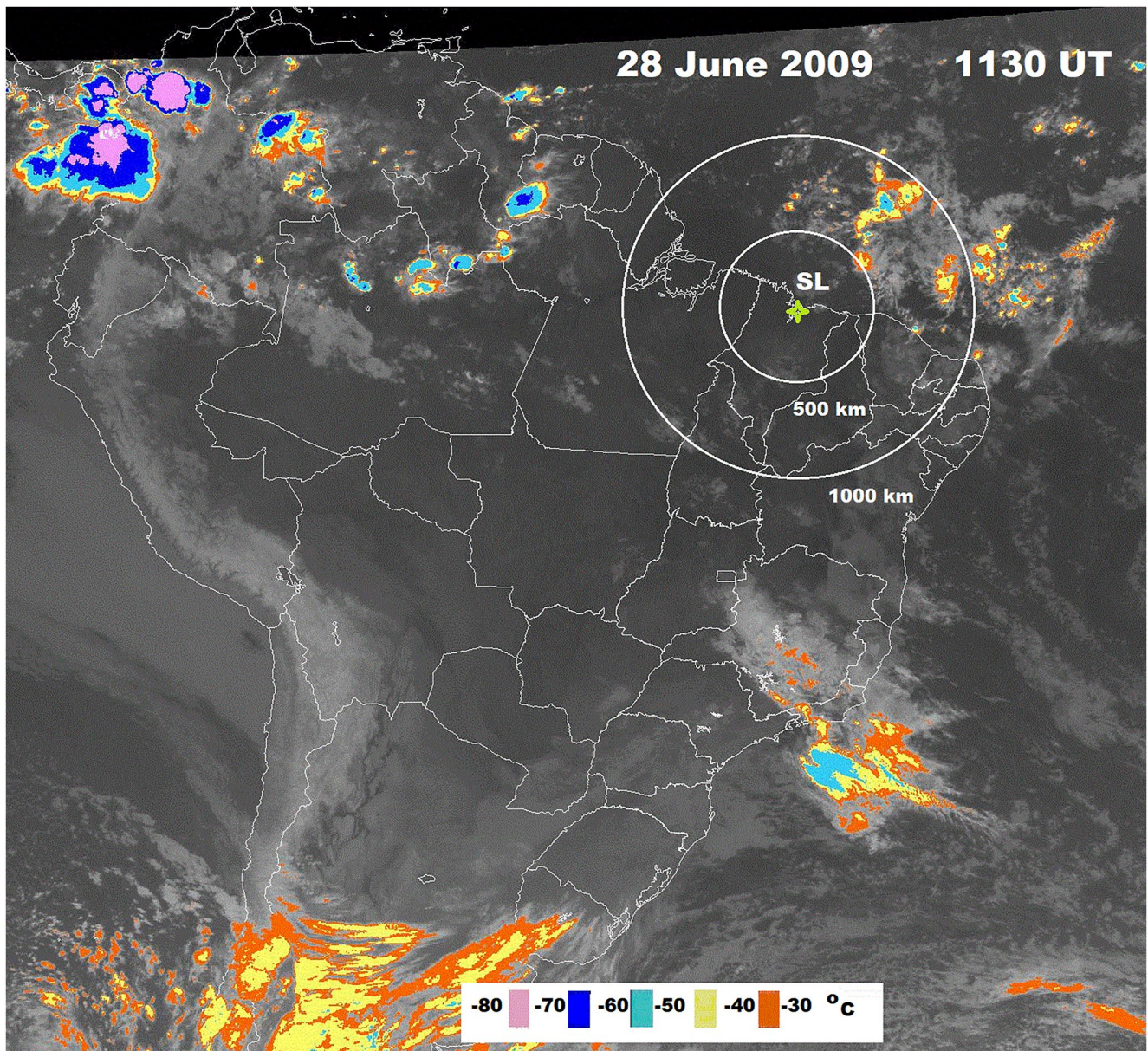
Figure 4. Image from GOES satellite at 11:30 UT on 28 June 2009 showing the presence of convective zones near São Luis.

EEJ over Peru does not present any decrease as shown in Figure 1. These important features lead us to believe that the phenomena responsible for the abrupt changes over the Brazilian equatorial region had a local origin, such as gravity waves activity for example, and not a global one as should be in the case of penetration electric fields. As can be seen in an image from the GOES-10 satellite (http://satelite.cptec.inpe.br/acervo/goes.formulario.logic?i=br) in Figure 4, there are tropospheric convective zones near SL that could justify the presence of such GWs. It is possible to observe convective zones with temperatures near ∼−50°C and −60°C within a radius greater than 500 km north-east of São Luis and the 1600 km radius north-west of São Luis some hours before the CEJ occurrence (11:30 UT on 28 June).

To investigate the possible influence of the GWs in the case studied here, we use the Fast Fourier Transform (FFT) to reconstruct the *F* layer height variation considering periodicities higher than 30 min and a temporal rate of 90 s (the Digisondes' temporal acquisition rate was 15 min for CP and FZ and 10 min for SL) as can be seen in Figure 5. This analysis can help us to visualize the downward phase progression attributed to gravity waves in the ionosonde data. In this case, the *F* layer true heights at several plasma frequencies at 0.1 MHz intervals starting at
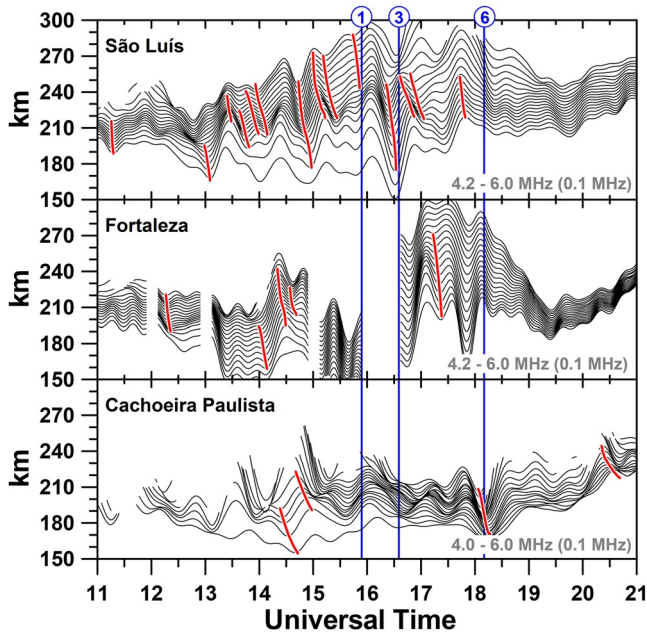
Figure 5. FFT reconstruction of the altitudinal variation of different plasma frequencies for SL, FZ, and CP (from the top to the bottom panel). The red lines highlight the phase progression with altitude and time. The numbers of the vertical blue lines denotes the time position of the event shown in Figure 3 (panel a).

4.2 MHz up to 6.0 MHz for São Luis and Fortaleza, and at 4.0–6.0 MHz for Cachoeira Paulista were used. The numbers 1, 3, and 6 indicated in Figure 5 correspond to the same numbers as in Figure 3 and refer to the time before, during and after the CEJ, respectively. It can be clearly noted that the regions near the equator (SL and FZ) were very disturbed by the gravity waves including the period before (number 1), during (number 2–5), and after the CEJ occurrence (number 6–8), as seen in the downward phase propagation of the altitude along the time (slanted red lines). It is important to mention that to make the FFT of the altitudinal variation of different plasma frequencies it was necessary to choose frequencies situated above the E, Es, and F_1 layer critical frequencies ($f > 4.2$ MHz over SL and FZ, and $f > 4.0$ MHz over CP) in order to avoid discontinuity of the signal (sharp jump in altitude of the reflected signal by the ionosphere), and this was possible only after 11:00 UT. Evidences of wave-like disturbances are also observed in the dTEC parameter few hours before and after the CEJ over some stations close to SL (not shown here).

As shown in Figure 2, hmF_2 over SL and FZ presented lower values when compared to the reference curve in the period that preceded the CEJ occurrence. At the same time, the EEJ on this day was clearly weaker when compared to the average value of quiet days. As the peak height of the F_2 layer and the intensity of EEJ are controlled by the zonal electric field (Ez), and as the GWs can affect the ionospheric electric fields (Kelley et al., 2009), it is possible that the day-to-day variability in Ez added to the strong GW activity as evidenced in Figure 5, could be responsible for the weakening and the subsequent reversal of the EEJ, and consequently the anomalous changes in the F layer. The foF_2 parameter fluctuation over FZ between 11:00 UT and 16:00 UT (see panel c of Figure 2) could also have been modulated by the GW propagation.

As mentioned previously, convective zones with temperatures near $\sim -50°C$ and $-60°C$ were observed near São Luis some hours before the CEJ occurrence (1130 UT on 28 June) and also on the previous day, especially at the end of the day. Vadas et al. (2009) reported that GWs could take ~3–24 hr to reach the lower thermosphere. Venkateswara Rao et al. (2011), on the other hand, suggested a time delay of ~1–15 hr between the peak of deep convection and propagating GWs in the lower thermosphere. Therefore, it is possible that the convection of upward propagating GWs excited by tropospheric convection regions could be responsible for the changes observed in the Brazilian equatorial region on 28 June 2009. As reported by Shume et al. (2014), gravity waves could modulate electric fields in the electrojet. They observed a similar weakening in the EEJ during daytime probably due to GWs, but in their case, the reversal of EEJ was not observed. Due to the strong coupling between the E and F regions that exists during daytime, and considering we are referring to the period of deep minimum in solar activity, any variation in the E region electric field could cause variability in the F region. This is clearly observable in the results presented here since all the changes in the E region were accompanied by an anomalous change in the F layer.

A careful analysis of the ionograms over the sectors studied here also reveals interesting characteristics that resemble the manifestation of GW propagation, such as the forking trace, perturbation in F layer traces, and the F_3 layer formation over the equatorial region. Figure 6 illustrates the complete sequence of the ionograms over SL during this event of 28 June from 14:00 UT to 19:50 UT. It can be noted a well-defined bifurcation at the F layer, which started with a weak inflection around ~5.5 MHz at 14:10 UT that evolved into three stratifications at ~5.0, 6.1, and 6.2 MHz in ordinary trace at 15:00 UT. Such stratifications can be easily identified through the slanted blue arrows indicated in the ionograms at these times. Additionally, around this time and some hours before, a manifestation of GW was clearly seen, as indicated by the downward phase propagation in the isodensity lines over SL in Figure 5. At the moment in which the decrease in EEJ started (16:20 UT), the stratification in the high-frequency end in the F_2b layer evolved to what is known as forking trace produced by GWs (Abdu et al., 1982). A more complete nature of the GW is clearly observed in the ionogram traces at 16:30 UT when the
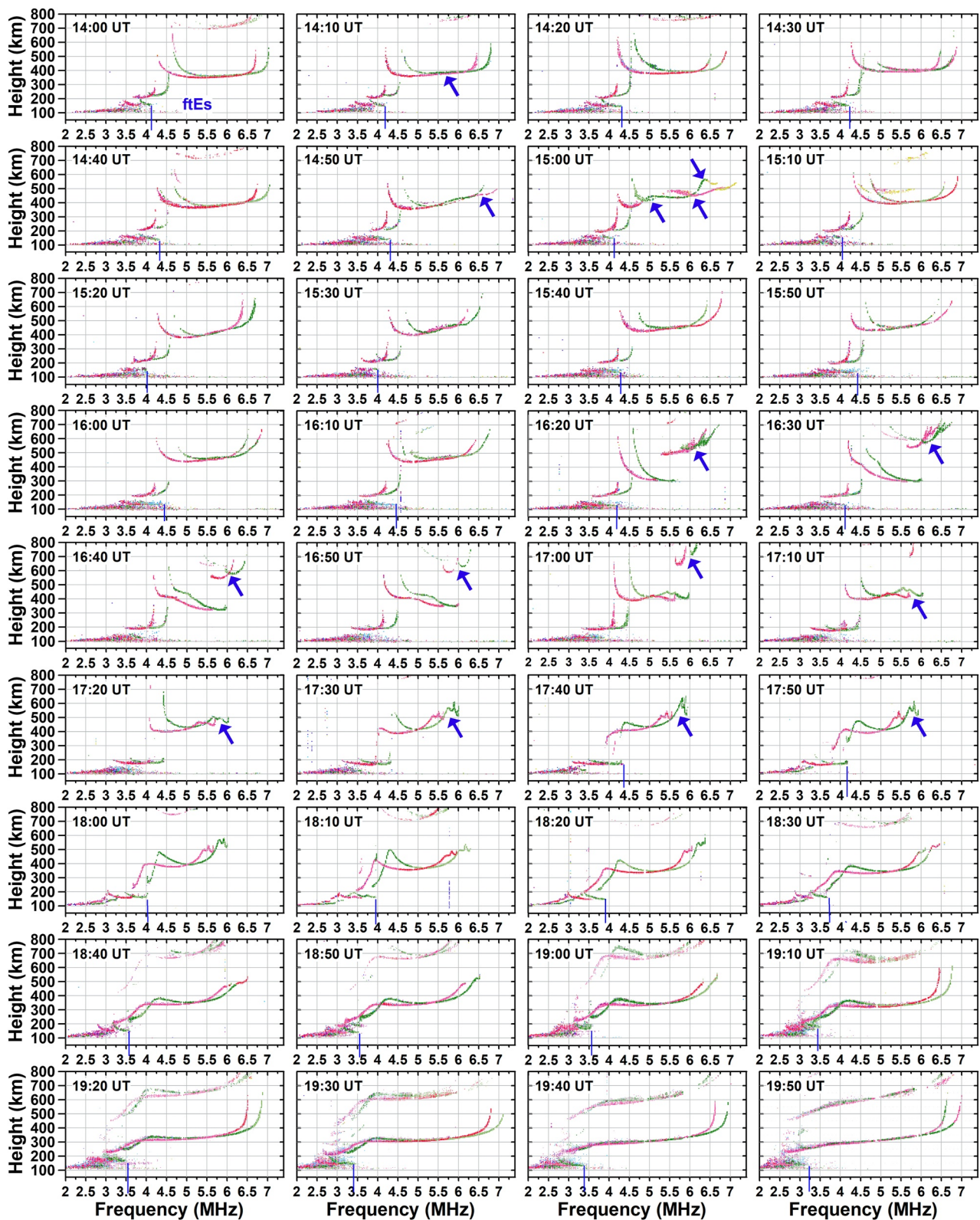
Figure 6. Ionogram sequence over SL on 28 June 2009.

GW disturbance seems to propagate down to what we considered as the F_2a layer trace (see the cusp at around 5 MHz indicated by the vertical blue arrow in Figure 6). Starting from 16:40 UT, we notice the further evolution of the F layer. It appears that the top layer with $h'F_2b$ of ~520 km was lifted upward leading its disappearance beyond the ionogram height range (of 800 km), by 17:10 UT.

Regarding the Es layers over SL on 28 June, it is possible to note that the ongoing Es layer located at 150 km (14:00 UT) presented a downward movement and probably merged with the q-type Es layer in development (16:40 UT) during the period of decrease of EEJ intensity. As indicated by the vertical blue line in Figure 6, a slight fluctuation occurred in the height and top frequency of such layer, which could be associated with the GW propagation. On the other hand, the Esq layer (100 km) weakened during the reversal of EEJ, until it was totally blocked at 17:50 UT. This weakening and subsequent interruption of Esq maybe be related by CEJ occurrence (see e.g., Resende & Denardini, 2012; and Denardini et al., 2009). Another interesting characteristic is that throughout this process of strong changes in EEJ behavior, the $F1$ layer was transforming and detached from the upper layer (F_2a) at 17:40 UT giving origin to a layer named as an intermediate layer (see dos Santos et al., 2019) at about ~150 km.

4. Conclusions

This work presented an unusual and very interesting behavior of the F layer over the Brazilian equatorial sector during a strong CEJ event probably caused by GW occurrence. The period studied is the deep solar minimum of 2009, when the ionosphere presented a very special condition, where the tides and waves originating in the lower atmosphere were able to show their effects on the thermosphere and ionosphere more easily (see e.g., Balan et al., 2012). The main findings of this work are summarized below:

1. The weakening of daytime EEJ and its subsequent reversal to westward occurred in the presence of intense GW activity;
2. The ionospheric F_2 layer trace was stratified into two layers under a CEJ event probably due to the GW propagation;
3. The ionosphere remained strongly disturbed for about 2 hours since the reversal of the EEJ up to their return to the quiet time, and;
4. GWs signatures were detected in the ionosphere up to 3 hours prior to the CEJ event; and they occurred during the whole period of the CEJ event.

Additional studies need to be done in order to understand better all the electrodynamic processes involved in this event, however, at this moment, we consider the GW as the more plausible hypothesis to explain the observed variations over São Luís.

Data Availability Statement

The indices Sym-H, Bz, and the AE were obtained from the website https://omniweb.gsfc.nasa.gov/form/omni_min.html (last access: 13 July 2021). The ionosonde data used here can be found in Zenodo (https://doi.org/10.5281/zenodo.6481549). An image from GOES-10 satellite was obtained from the website http://satelite.cptec.inpe.br/acervo/goes.formulario.logic?i=br.

References

Abdu, M., Kherani, A. E. A., Batista, I. S., & Sobral, J. H. A. (2009). Equatorial evening prereversal vertical drift and spread F suppression by disturbance penetration electric fields. *Geophysical Research Letters*, *36*(19), L19103. https://doi.org/10.1029/2009GL039919

Abdu, M. A. (2012). Equatorial spread F development and quiet time variability under solar minimum conditions. *Indian Journal of Radio and Space Physics*, *42*, 168–183.

Abdu, M. A., Batista, I. S., Kantor, I. J., & Sobral, J. H. A. (1982). Gravity wave induced ionization layers in the night F-region at low latitudes. *Journal of Atmospheric and Terrestrial Physics*, *44*(9), 759–767. https://doi.org/10.1016/0021-9169(82)90004-6

Abdu, M. A., Batista, P. P., Batista, I. S., Brum, C. G. M., Carrasco, A. J., & Reinisch, B. W. (2006). Planetary wave oscillations in mesospheric winds, equatorial evening prereversal electric field and spread F. *Geophysical Research Letters*, *33*(7), L07107. https://doi.org/10.1029/2005GL024837

Abdu, M. A., & Brum, C. G. M. (2009). Electrodynamics of the vertical coupling processes in the atmosphere–ionosphere system of the low latitude region. *Earth Planets and Space*, *61*(4), 385–395. https://doi.org/10.1186/BF03353156

Abdu, M. A., Denardini, C. M., Sobral, J. H. A., Batista, I. S., Muralikrishna, P., Iyer, K. N., et al. (2003). Equatorial electrojet 3-m irregularity dynamics during magnetic disturbances over Brazil: Results from the new VHF radar at São Luís. *Journal of Atmospheric and Solar-Terrestrial Physics*, *65*(14–15), 1293–1308. https://doi.org/10.1016/j.jastp.2003.08.011

Abdu, M. A., Nogueira, P. A. B., Souza, J. R., Batista, I. S., Dutra, S. L. G., & Sobral, J. H. A. (2017). Equatorial electrojet responses to intense solar flares under geomagnetic disturbance time electric fields. *Journal of Geophysical Research: Space Physics*, *122*, 3570–3585. https://doi.org/10.1002/2016JA023667

Abdu, M. A., Ramkumar, T. K., Batista, I. S., Brum, C. G. M., Takahashi, H., Reinisch, B. W., & Sobral, J. H. A. (2006b). Planetary wave signatures in the equatorial atmosphere-ionosphere system, and Mesosphere- *E-* and *F*-region coupling. *Journal of Atmospheric and Solar-Terrestrial Physics*, *68*(3–5), 509–522. https://doi.org/10.1016/j.jastp.2005.03.019

Balan, N., Chen, C. Y., Rajesh, P. K., Liu, J. Y., & Bailey, G. J. (2012). Modeling and observations of the low latitude ionosphere plasmasphere system at long deep solar minimum. *Journal of Geophysical Research*, *117*, A08316. https://doi.org/10.1029/2012JA017846

Batista, I. S., De Paula, E. R., Abdu, M. A., Trivedi, N. B., & Greenspan, M. E. (1991). Ionospheric effects of the March 13, 1989, magnetic storm at low and equatorial latitudes. *Journal of Geophysical Research*, *96*(A8), 13943–13952. https://doi.org/10.1029/91JA01263

Brum, C. G. M., Aponte, N., Santos, A. M., & Sulzer, M. (2021). Responses of the topside ion fractions concentration over the Arecibo Observatory to solar and geomagnetic activity for the summer period. In *2021 XXXIVth general assembly and scientific symposium of the international union of radio science (URSI GASS)* (pp. 01–03). https://doi.org/10.23919/URSIGASS51995.2021.9560602

Budden, K. G. (1985). *Propagation of radio waves*. Cambridge University Press.

Denardini, C. M., Abdu, M. A., Aveiro, H. C., Resende, L. C. A., Almeida, P. D. S. C., Olivio, E. P. A., et al. (2009). Counter electrojet features in the Brazilian sector: Simultaneous observation by radar, digital sounder and magnetometers. *Annales Geophysicae*, *27*(4), 1593–1603. https://doi.org/10.5194/angeo-27-1593-2009

Dos Santos, Â. M., Batista, I. S., Abdu, M. A., Sobral, J. H. A., Souza, J. R., & Brum, C. G. M. (2019). Climatology of intermediate descending layers (or 150 km echoes) over the equatorial and low-latitude regions of Brazil during the deep solar minimum of 2009. *Annales Geophysicae*, *37*(6), 1005–1024. https://doi.org/10.5194/angeo-37-1005-2019

Fambitakoye, O., Mayuad, P. N., & Richmond, A. D. (1976). Equatorial electrojet and regular variations S_R-III: Comparison of observations with a physical model. *Journal of Atmospheric and Terrestrial Physics*, *38*, 113–121.

Fritts, D. C., Vadas, S. L., Riggin, D. M., Abdu, M. A., Batista, I. S., Takahashi, H., et al. (2008). Gravity wave and tidal influences on equatorial spread F based on observations during the Spread F Experiment (SpreadFEx). *Annales Geophysicae*, *26*(11), 3235–3252. https://doi.org/10.5194/angeo-26-3235-2008

Garzón, D. P., Brum, C. G. M., Echer, E., Aponte, N., Sulzer, M. P., González, S. A., et al. (2011). Response of the topside ionosphere over Arecibo to a moderate geomagnetic storm. *Journal of Atmospheric and Terrestrial Physics*, *73*(11–12), 1568–1574. https://doi.org/10.1016/j.jastp.2011.02.016

Ghosh, P., Ramkumar, T. K., Patra, A. K., Sharma, S., & Pavan Chaitanya, P. (2019). Vertical coupling from the lower atmosphere to the ionosphere: Observations inferred from Indian MST radar, GPS radiosonde, ionosonde, magnetometer, OLR (NOAA), and SABER/TIMED instrument over Gadanki. *Journal of Geophysical Research: Space Physics*, *124*, 489–503. https://doi.org/10.1029/2018JA025897

Gurubaran, S. (2002). The equatorial counter electrojet: Part of a worldwide current system. *Geophysical Research Letters*, *29*(9), 1337–1351-4. https://doi.org/10.1029/2001gl014519

Kelley, M. C. (1989). *The Earth's ionosphere* (p. 487). Academic Press.

Kelley, M. C., Ilma, R. R., & Crowley, G. (2009). On the origin of pre-reversal enhancement of the zonal equatorial electric field. *Annales Geophysicae*, *27*(5), 2053–2056. https://doi.org/10.5194/angeo-27-2053-2009

Kelley, M. C., Makela, J. J., Chau, J. L., & Nicolls, M. J. (2003). Penetration of the solar wind electric field into the magnetosphere/ionosphere system. *Geophysical Research Letters*, *30*(4), 1158. https://doi.org/10.1029/2002GL016321

Kikuchi, T., Hashimoto, K. K., & Nozaki, K. (2008). Penetration of magnetospheric electric fields to the equator during a geomagnetic storm. *Journal of Geophysical Research*, *113*, A06214. https://doi.org/10.1029/2007JA012628

Kikuchi, T., Pinnock, M., Rodger, A., Luhr, H., Kitamura, T., Tachihara, H., et al. (2000). Global evolution of a substorm-associated DP2 current system observed by Super DARN and magnetometers. *Advances in Space Research*, *26*(960), 121–124. https://doi.org/10.1016/s0273-1177(99)01037-6

Koucká Knížová, P., Laštovička, J., Kouba, D., Mošna, Z., Podolská, K., Potužníková, K., et al. (2021). Ionosphere influenced from lower-lying atmospheric regions. *Frontiers in Astronomy and Space Sciences*, *8*, 54. https://doi.org/10.3389/fspas.2021.651445

Raghavarao, R., & Anandarao, B. G. (1980). Vertical winds as a plausible cause for equatorial counter electrojet. *Geophysical Research Letters*, *7*(5), 357–360. https://doi.org/10.1029/GL007i005p00357

Ratcliffe, J. A. (1959). *The magneto-ionic theory and its applications to the ionosphere*. Cambridge University Press.

Resende, L. C. A., & Denardini, C. M. (2012). Equatorial sporadic E-layer abnormal density enhancement during the recovery phase of the December 2006 magnetic storm: A case study. *Earth Planets and Space*, *64*(4), 345–351. https://doi.org/10.5047/eps.2011.10.007

Santos, A. M., Abdu, M. A., Sobral, J. H. A., Koga, D., Nogueira, P. A. B., & Candido, C. M. N. (2012). Strong longitudinal difference in ionospheric responses over Fortaleza (Brazil) and Jicamarca (Peru) during the January 2005 magnetic storm, dominated by northward IMF. *Journal of Geophysical Research*, *117*, A08333. https://doi.org/10.1029/2012JA017604

Santos, A. M., Abdu, M. A., Souza, J. R., Sobral, J. H. A., & Batista, I. S. (2016). Disturbance zonal and vertical plasma drifts in the Peruvian sector during solar minimum phases. *Journal of Geophysical Research: Space Physics*, *121*, 2503–2521. https://doi.org/10.1002/2015JA022146

Santos, A. M., Abdu, M. A., Souza, J. R., Sobral, J. H. A., Batista, I. S., & Denardini, C. M. (2016). Storm time equatorial plasma bubble zonal drift reversal due to disturbance Hall electric field over the Brazilian region. *Journal of Geophysical Research: Space Physics*, *121*, 5594–5612. https://doi.org/10.1002/2015JA022179

Sastri, J. H., Rao, J. V. S. V., & Ramesh, K. B. (1993). Penetration of polar electric field to the nightside dip equator at times of geomagnetic sudden commencements. *Journal of Geophysical Research*, *98*(A10), 17517–17523. https://doi.org/10.1029/93JA00418

Shume, E. B., Rodrigues, F. S., Mannucci, A. J., & de Paula, E. R. (2014). Modulation of equatorial electrojet irregularities by atmospheric gravity waves. *Journal of Geophysical Research: Space Physics*, *119*, 366–374. https://doi.org/10.1002/2013JA019300

Soares, G., Yamazaki, Y., Matzka, J., Pinheiro, K., Morschhauser, A., Stolle, C., & Alken, P. (2018). Equatorial counter electrojet longitudinal and seasonal variability in the American sector. *Journal of Geophysical Research: Space Physics*, *123*, 9906–9920. https://doi.org/10.1029/2018JA025968

Sobral, J. H. A., Abdu, M. A., Gonzalez, W. D., Tsurutani, B. T., Batista, I. S., & Gonzalez, A. L. C. (1997). Effects of intense storms and substorms on the equatorial ionosphere/thermosphere system in the American sector from ground-based and satellite data. *Journal of Geophysical Research*, *102*(A7), 14305–14313. https://doi.org/10.1029/97JA00576

Sobral, J. H. A., Abdu, M. A., Yamashita, C. S., Gonzalez, W. D., de Gonzalez, A. C., Batista, I. S., et al. (2001). Responses of the low-latitude ionosphere to very intense geomagnetic storms. *Journal of Atmospheric and Solar-Terrestrial Physics*, *63*(9), 965–974. https://doi.org/10.1016/S1364-6826(00)00197-8

Somayajulu, V. V., Cherian, L., Rajeev, K., Ramkumar, G., & Reddy, C. R. (1993). Mean winds and tidal components during counter electrojet events. *Geophysical Research Letters*, *20*(14), 1443–1446. https://doi.org/10.1029/93GL00088

Vadas, S. L., & Fritts, D. C. (2006). Influence of solar variability on gravity wave structure and dissipation in the thermosphere from tropospheric convection. *Journal of Geophysical Research*, *111*, A10S12. https://doi.org/10.1029/2005JA011510

Vadas, S. L., & Liu, H. (2009). Generation of large-scale gravity waves and neutral winds in the thermosphere from the dissipation of convectively generated gravity waves. *Journal of Geophysical Research*, *114*, A10310. https://doi.org/10.1029/2009JA014108

Vadas, S. L., Taylor, M. J., Pautet, P. D., Stamus, P. A., Fritts, D. C., Liu, H. L., et al. (2009). Convection: The likely source of the medium-scale gravity waves observed in the OH airglow layer near Brasilia, Brazil, during the SpreadFEx campaign. *Annales Geophysicae*, *27*(1), 231–259. https://doi.org/10.5194/angeo-27-231-2009

Venkatesh, K., Fagundes, P. R., Prasad, D. S. V. V. D., Denardini, C. M., de Abreu, A. J., de Jesus, R., & Gende, M. (2015). Day-today variability of equatorial electrojet and its role on the day-to-day characteristics of the equatorial ionization anomaly over the Indian and Brazilian sectors. *Journal of Geophysical Research: Space Physics*, *120*, 9117–9131. https://doi.org/10.1002/2015JA021307

Venkatesh, K., Tulasi Ram, S., Fagundes, P. R., Seemala, G. K., & Batista, I. S. (2017). Electrodynamic disturbances in the Brazilian equatorial and low-latitude ionosphere on St. Patrick's Day storm of 17 March 2015. *Journal of Geophysical Research: Space Physics*, *122*, 4553–4570. https://doi.org/10.1002/2017JA024009

Venkateswara Rao, N., Shibagaki, Y., & Tsuda, T. (2011). Diurnal variation of short-period (20–120 min) gravity waves in the equatorial Mesosphere and Lower thermosphere and its relation to deep tropical convection. *Annales Geophysicae*, *29*(4), 623–629. https://doi.org/10.5194/angeo-29-623-2011

Vineeth, C., Pant, T. K., & Hossain, M. M. (2012). Enhanced gravity wave activity over the equatorial MLT region during counter electrojet events. *Indian Journal of Space and Radio Physics*, *41*, 258–263.

Yiğit, E., & Medvedev, A. S. (2010). Internal gravity waves in the thermosphere during low and high solar activity: Simulation study. *Journal of Geophysical Research*, *115*, A00G02. https://doi.org/10.1029/2009JA015106

Yusupov, K. M., & Bakhmetieva, N. V. (2021). Sporadic E layer with a structure of double cusp in the vertical sounding ionogram. *Atmosphere*, *12*(9), 1093. https://doi.org/10.3390/atmos12091093